Verification of Experimentally Determined Permeability and Form Coefficients of Al_2O_3 Ceramic Foam Filters (CFF) at High and Low Flow Velocity Using a CFD Model

Massoud Hassanabadi[1], Mark W. Kennedy[1], Shahid Akhtar[2], and Ragnhild E. Aune[1]

[1]Dept. of Materials Science and Engineering, Norwegian University of Science and Technology (NTNU), Trondheim, Norway
[2]Hydro Aluminium, Karmøy Primary Production, Håvik, NORWAY

Corresponding author: massoudh@ntnu.no (+47) 48345692

Keywords: Ceramic Foam Filters (CFFs), Permeability, Form coefficient, COMSOL Multiphysics®

Abstract
Filtration using Ceramic Foam Filters (CFFs) is a method widely used to separate inclusions from molten aluminium. In the present work, the specific permeability and form drag coefficients of nominal 50 mm thick commercial Al_2O_3-based CFFs, of grades 30, 50, 65 and 80, have been calculated from pressure drop experiments using high (60-500 mm·s^{-1}) and low (0.2-10 mm·s^{-1}) water velocities. Moreover, 2D axial symmetric Computational Fluid Dynamic (CFD) models have been developed, using COMSOL Multiphysics® to validate the experimental results. The empirically obtained values were defined as global parameters used to model the pressure, as well as the velocity fields in the water pipes and in the CFFs. The modelled pressure drop over the filter thickness for the high water velocity experiments showed < ±1 % deviation from the corresponding experimental results for all CFF grades. Moreover, the developed model also showed good agreement with the experimental results obtained from the low water velocity experiments, where the deviation of the pressure drop for the CFF samples of grade 30, 50 and 65 were ≤ ±4.6 % and for CFF samples of grade 80 ≤ ± 13.4 %.

1. Introduction

Removal of inclusions is a crucial step in the melt treatment process of molten aluminium and its alloys. Over the years filtration, using Ceramic Foam Filters (CFFs) as the filtration media, has proven to be a simple, reliable and cost-effective method that allows the aluminium producers to meet the ever-increasing demands of their customers in regards to high purity aluminium.

It is a well-known fact that in the initial stages of the filtration process it is important to prime the filter, *i.e.* the filter must be wetted by the molten aluminium, and the air present in the filter pores and on the surface of the filter must be replaced by molten metal. To secure the conditions needed for priming the filter, a metal-static head, *i.e.* priming head, is required. The priming head needed in each specific case depends on the metal temperature, the pre-heat temperature and uniformity, the incoming metal composition and quality, the molten metal velocity, the pre-filter treatments, as well as the cell size (permeability) of the filter [1-3].

Permeability is the structural characteristic of a porous media, and it can be estimated by measuring the resulting presser drop over the filter thickness when a fluid media flows through its tortuous structure. In regards to CFFs used for filtration of aluminium, the operating metal head needed to secure a constant flow of metal through the filter is directly influenced by the permeability. In other words, the specific permeability and form drag coefficients of Al_2O_3-based CFFs are important properties that needs to be defined for different grades of CFFs, as well as for different flow velocities.

For the calculation of the specific permeability and form drag coefficients of CFFs, many of the empirical studies reported in literature are based on experimental activities using water as the fluid media at flow rates much higher than the industrially reported molten aluminium velocity, *i.e.* 2-15 mm·s^{-1} for production of billets and during continuous casting [2-5]. As a result, there is a lack of experimental information in regards to these properties for CFFs obtained at low flow velocities.

The main objective of the present study is to model the pressure differences over a porous media having the same porosity as Al_2O_3-based CFFs of grade 30, 50, 65 and 80, and further validate the results obtained from the presser drop experiments performed with water at high and low fluid velocities using COMSOL Multiphysics®.

2. Theory

The Hazen-Darcy law (mainly referred to as the Darcy's law) describes the fluid flow in porous media at very low fluid velocities:

$$-\nabla P = \frac{\mu}{k}\mathbf{u} \qquad (1)$$

where ∇P is the pressure gradient ($kg \cdot m^{-2} \cdot s^{-2}$ or $Pa \cdot m^{-1}$), μ the dynamic viscosity ($kg \cdot m^{-1} \cdot s^{-1}$), k the intrinsic permeability (m^2), and $\mathbf{u}$ the fluid velocity vector (superficial velocity) ($m \cdot s^{-1}$) [6]. Eq. 1 is valid essentially for incompressible and creeping flow of a Newtonian fluid through a relatively long, uniform and isotropic porous media [7]. The use of Darcy's law is, however, not the most suitable approach for predicting the pressure drop through a porous media, as it cannot explain the deviation from linearity as the fluid velocity increases [6-8]. As a result, Brinkman suggested a modification of Darcy's law to compensate for the nonlinearity, *i.e.* the addition of the Laplacian term of Stokes flow (creeping flow) to Eq. 1:

$$\nabla P = -\frac{\mu}{k}\mathbf{u} + \mu_e \nabla^2 \mathbf{u} \qquad (2)$$

where μ_e is the effective (apparent) viscosity ($kg \cdot m^{-1} \cdot s^{-1}$). In regards to the Stokes flow, it is a fluid flow where the inertial forces in the system are neglected, as they are very small compared to the viscous forces [7-9]. In other words, the Laplacian term adds the diffusive transport of momentum by means of the viscous shear stresses to Eq. 1. It should in this context be mentioned that the effective viscosity, μ_e in comparison to the dynamic viscosity, μ, is a porosity dependent parameter, but Brinkman considered them to be equal as the actual relationship between them was unknown. This assumption is still today used in many studies related to fluid flow through porous media [9, 10].

The nonlinearity of the so-called non-Darcy fluid is also often explained by the addition of a quadratic term to the Darcy's law to generalize the flow equation. The Forchheimer equation, also known as the Forchheimer-extended Darcy equation and the Hazen-Dupuit-Darcy equation, is today the globally accepted equation valid for porous media of finite length and with a specific cross-sectional area, *i.e.*:

$$-\nabla P = \frac{\mu}{k}\mathbf{u} + \beta\rho\mathbf{u}^2 \qquad (3)$$

where β (m^{-1}) is the form drag coefficient and ρ the fluid density ($kg \cdot m^{-3}$) [6, 7]. The first and second terms on the right-hand side of Eq. 3 represent the lumped viscous and the lumped form drag effects within the permeable medium, respectively. The form drag force is the pressure gradient needed to overcome the liquid-solid interactions taking place in the system [8].

3. Experimental

The permeability and form drag coefficients of commercial Al_2O_3-based CFFs of grade 30, 50, 65 and 80 were determined by measuring the pressure drop associated with several different high (60-500 $mm \cdot s^{-1}$) and low (0.2-10 $mm \cdot s^{-1}$) water velocities at a temperature ranging from 281 to 284 K. In Fig. 1 (a) and (b) a schematic drawing of the experimental set-up used for the presser drop measurements, as well as the exploded 3D CAD drawing of the sample housing, are presented.

Cylindrical CFF samples with 50 mm nominal diameter were cut from industrial size CFFs by using a core drill, and their weight and true dimensions measured after drying at 423 K for 12 hours. To prevent the textured/dimpled axial surface of the samples to affect the experimental results, the outer wall of each sample was sealed with a thin layer (1-2 mm) of SuperFix glue wrapped in a sheet of cellulose. High viscosity silicon grease was further used to smoothen the surface before the sample was pressed tightly into the holder leaving no gaps/channels to allow fluid (water) to bypass the filter.

The pressure difference before and after the filter was measures at high and low water velocities using two different pressure transducers, *i.e.* (1) a DF2R 100 mbar and (2) a DF2 1 bar pressure transducer. The DF2R was calibrated to an output from 0 to 10 V with a resolution of 0.001 V, corresponding to a ± 0.03 % uncertainty of the measured pressure. The DF2 was calibrated from 4 to 20 mA with a resolution of 0.001 mA and a ± 0.03% uncertainty in the measured pressure. The output voltage and ampere signals from the pressure transducers were

automatically logged using a FLUKE 289 True RMS Multimeter with a resolution of 0.001mV and a 0.025% mV (0.05% mA DC) uncertainty relative to the reading.

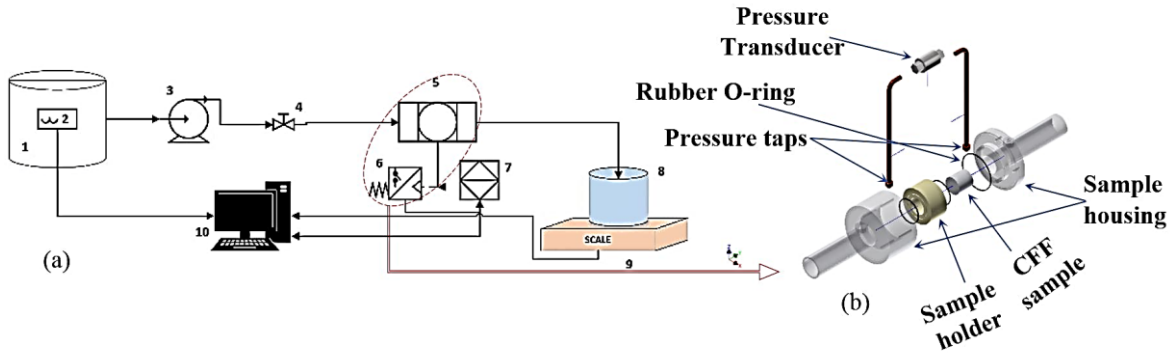

Fig. 1- (a) Schematic drawing of the experimental presser drop set-up: 1. Water reservoir, 2. Thermocouple, 3. Centrifugal pump, 4. Control valve, 5. Sample housing and CFF sample, 6. Pressure transducer, 7. Volt-Ohm-milliammeter, 8. Collecting tank, 9. Digital scale, 10. Computer for data logging, and (b) Exploded 3D CAD drawing of the sample housing.

The mass flow rate, Q, of water through the CFF sample was determined from the mass of the accumulated water automatically logged every second. Two different digital scales, *i.e.* one with a resolution of 0.02 kg and maximum capacity of 60 kg, and the other with a resolution of 0.1 mg and maximum capacity of 220 g were used. The superficial velocity, **u**, was determined from the mass flow rate, Q, the cross-sectional area of the sample, A_s, and the density of water, ρ.

4. Numerical Model

A numerical 2D axisymmetric model was developed using COMSOL Multiphysics® version 5.3 to validate the permeability and form drag coefficients experimentally determined in the present study. The size of the model geometry and all the defined parameters were set according to the actual dimensions of the experimental set-up and the measured and/or calculated parameters obtained from the experiments. The porous media (CFF), the inlet and outlet sections of the model geometry, the computational mesh, and the boundary conditions are presented in Fig. 2. "Normal" triangular Physics-controlled mesh was used to reduce the execution time, as finer mesh proved not to result in any significant improvement of the results. It should, however, be noted that multiple boundary layers were inserted in the mesh in zones of high gradients to minimize numerical errors. Based on the excellent sealing in the gap between the outer wall of the CFFs and the sample holder's inner wall, no fluid bypassing had to be considered.

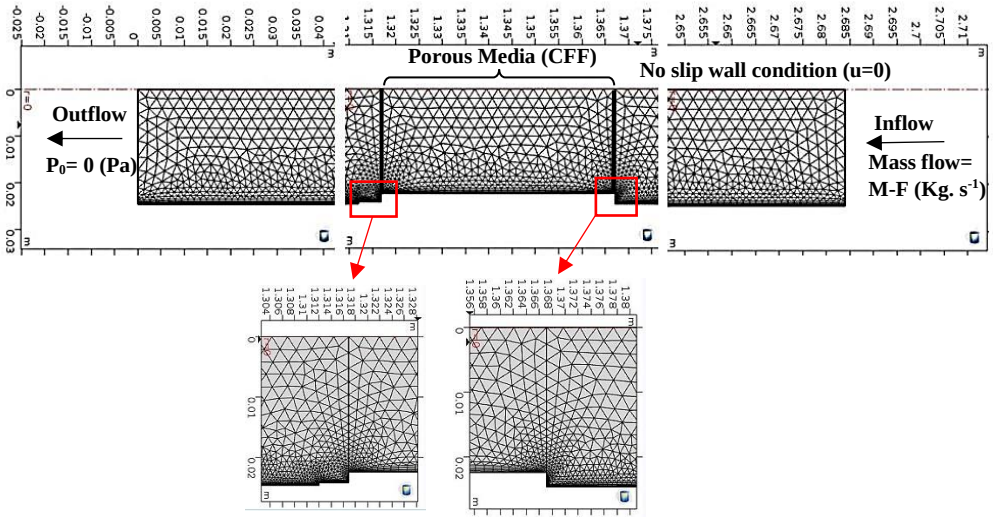

Fig. 2- The geometry, computational mesh and boundary conditions of the numerical 2D axisymmetric model.

The following basic assumptions were made:

1. stationary modelling conditions.
2. the porous media is isotropic and homogenous.

3. the water temperature, density and dynamic viscosity are constant.
4. the gravitational force can be neglected.
5. no fluid bypassing the sample.
6. the intrinsic permeability and the Forchheimer drag coefficients are constant in the range of measured mass flow velocities.

4.2. Governing Equations

Reynolds numbers for high and low flow velocities at the inlet of the water pipe were calculated to be in the range of 8-420 and 2200-20000, respectively, *i.e.* an initial laminar flow in the inlet of the water pipe was assumed followed by a turbulent flow. As a result, appropriate changes were made to the model formulation as described below.

For the turbulent flow the *"Turbulent Flow Algebraic yPlus"* interface coupled with the *"Porous Media"* domains were selected to simulate the flow in the water pipes and in the porous media at high velocities. The equations solved by the *"Turbulent Flow, Algebraic yPlus"* interface are the continuity equation for conservation of mass for incompressible fluids, *i.e.* Eq. 4, and the Reynolds-averaged Navier-Stokes (RANS) equation for conservation of momentum, *i.e.* Eq. 5:

$$\frac{\partial \rho}{\partial t} + \nabla.(\rho \mathbf{u}) = 0 \qquad (4)$$

$$\rho \frac{D\overline{u}_i}{Dt} = F_i - \frac{\partial \overline{P}}{\partial x_i} + \mu \Delta \overline{u}_i - \frac{\partial \overline{u_i' u_j'}}{\partial x_j} \qquad (5)$$

where ρ is the fluid density (kg·m^{-3}), ∇ the differential operator, $\mathbf{u}$ the velocity vector (m·s^{-1}), $\overline{u}_i$ the time-averaged mean velocity in the x_i direction, P the pressure (Pa), and μ the dynamic viscosity (kg·m^{-1}·s^{-1}) [4, 11-13]. The modelling of Reynolds stresses for solving the RANS equation is based on the Prandtl's mixing length theory and defining a two-layer algebraic model for the turbulent viscosity (eddy viscosity), which depends on the distance from the wall [12, 14]. By enabling the *"Porous Media"* domain check box, the *"Fluid and Matrix Properties"* node, the *"Mass Source"* node and the *"Forchheimer Drag"* node were all added to the *"Turbulent Flow, Algebraic yPlus"* interface that solves Eq. 4 for conservation of mass and Eq. 6 (the Brinkman-Dupuit-Forchheimer equation) for conservation of momentum [15]:

$$\nabla(\phi P) = -\frac{\mu}{k}\phi \mathbf{u}_i + \mu_e \nabla^2 \mathbf{u}_i + \beta \rho \phi^2 |\mathbf{u}_i| \mathbf{u}_i \qquad (6)$$

where ϕ is the effective (open) porosity (dimensionless), and $\mathbf{u}_i$ the average intrinsic velocity vector (m·s^{-1}). As the relation between the viscosity and the porosity is unknown the effective viscosity in Eq. 6 was assumed to be equal to the dynamic viscosity. The average intrinsic velocity is related to the superficial velocity according to the Dupuit–Forchheimer equation [9]:

$$\mathbf{u}_i = \frac{\mathbf{u}\ \text{(superficial velocity)}}{\phi\ \text{(Porosity)}} \qquad (7)$$

The Forchheimer drag coefficient, β_F, was determined using Eq. 8:

$$\beta_F = \rho \times \beta \qquad (8)$$

where β is the form drag coefficient (m^{-1}) that, in the present study, was determined from the pressure drop experiments.

The Reynolds numbers at the low flow velocity experiments were in the range of the laminar flow regime, *i.e.* Re < 1000 [12]. As a result, the pressure and velocity fields in the water pipes and in the porous media were modelled using the *"Laminar Flow"* interface coupled with the *"Porous Media"* domains, respectively. The governing equations for the laminar flow regime were the continuity equation for conservation of mass (Eq. 4), and the Navier-Stokes equation (Eq. 5) for conservation of momentum. However, the last term on the right hand side of Eq. 5, *i.e.* the Reynolds stresses, can be neglected, as there is no fluctuating component in the laminar flow.
The governing equations for solving the pressure and velocity fields in the porous media were Eq. 4 and Eq. 6. The third term on the right-hand side of Eq. 6, *i.e.* the form drag force, could also be neglected, as it is very small compare to the viscous forces. However, depending on the CFF grade and the fluid velocity range, the pressure drop may not increase linearly with the fluid velocity, which means that the form drag forces will influences the dissipation of energy. For the sake of precision of the model, the Forchheimer drag coefficient should therefore

be added to the low flow velocity models. This addition proved, however, to be most critical in the case of the lowest grade CFFs, *i.e.* grade 30.

5. Result and discussion

5.1. Pressure drop experiments

In Table 1 the average permeability and form drag coefficient of three 50 mm nominal diameter Al_2O_3-based CFF samples of grade 30, 50, 65 and 80, determined from high and low flow velocity pressure drop experiments, are presented. The experimental uncertainty was evaluated by error propagation and the maximum relative uncertainties found to be 0.67 % for the permeability and 13.5 % for the form drag coefficients at high flow velocity conditions, and 55.7 % for the permeability and 22% for the form drag coefficients at low flow velocity conditions. The maximum relative uncertainties of the velocity were evaluated to be 6 % and 57% for the high and low flow velocity pressure drop experiments, respectively. The higher relative experimental uncertainty in all the low flow velocity experiments is believed to be due to the fact that all measurements were performed very close to the minimum resolution of the digital scale used, which has a precision of 0.1 mg.

The comparison of the average permeability and form drag coefficients of each grade of CFF at high and low flow velocity conditions indicates that both parameters decrease as the flow velocity decreases. This observation supports the earlier findings by Dukhan *et. al.* [16] and K. Boomsma *et. al.* [17] that states that the permeability of metallic foams is a velocity related parameter. However, based on a statistical analysis (with 95% confidence interval) of the presently obtained permeability values at both high and low flow velocities it was established that the difference between the values were insignificant implying that the permeability is most likely not a velocity related parameter in the case of porous media.

Table 1: Empirically calculated permeability and form drag coefficients of three 50 mm nominal diameter Al_2O_3-based CFFs of grade 30, 50, 65 and 80 at high and low flow velocities.

	High Flow velocity		Low Flow velocity	
CFF Grade	**Permeability, k (m^2)**	**Form Drag, β (m^{-1})**	**Permeability k (m^2)**	**Form Drag β (m^{-1})**
30	9.19E-08	1.42E+03	5.32E-08	1.12E+03
50	2.22E-08	4.59E+03	1.89E-08	1.23E+03
65	1.44E-08	7.52E+03	1.15E-08	2.23E+03
80	8.61E-09	8.15E+03	6.55E-09	-

In Fig. 3 the pressure drop over the filter thickness, $\Delta P/h$, as a function of superficial velocity, u, for four Al_2O_3-based CFF samples of grade 30, 50, 65 and 80 at low flow velocities are presented. The equations seen in the figure corresponds to the linear and polynomial second order regression lines fitted to the experimental data points using the least squares method.

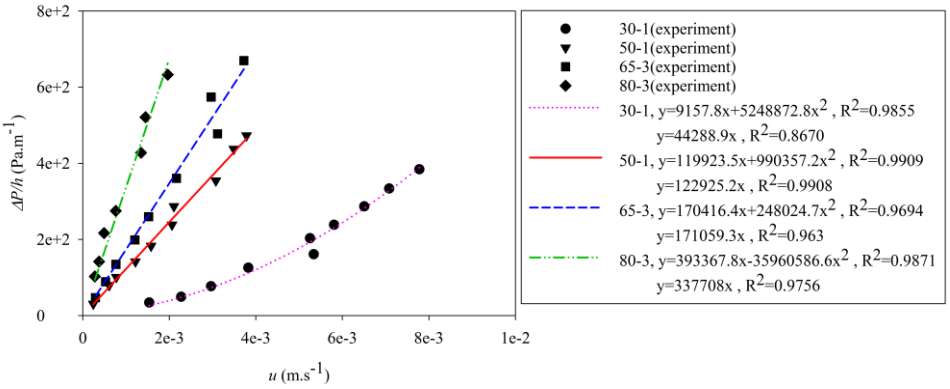

Fig. 3- The pressure drop over the CFF sample thickness, $\Delta P/h$, as a function of superficial velocity, u, of four CFF samples of grade 30, 50, 65 and 80 at low flow velocity.

As can be seen from Fig. 3 the CFF sample 1 of grade 30, *i.e.* sample 30-1, clearly exhibits a better fit with a polynomial regression line than with linear regression ($R^2_{Polynomial}$ = 0.9855 compare to R^2_{linear} = 0.8670). Therefore, despite the fact that the fluid velocity is very low, there are likely energy losses due to the existing

resistance of the CFF body against the fluid flow. Moreover, the CFF samples 50-1 and 65-3 showed fairly liner behaviour, but even in this case the polynomial regression exhibited a marginally better fit ($R^2_{Polynomial\ (50\text{-}1)}$ = 0.9909 compare to $R^2_{linear\ (50\text{-}1)}$ = 0.9908, and $R^2_{Polynomial\ (65\text{-}3)}$ = 0.9694 compare to $R^2_{linear\ (65\text{-}3)}$ = 0.963). This dose, however, not mean that the calculated form drag coefficients are significant, *i.e.* influence the dissipation of the energy inside the CFFs. Therefore, it was necessary to evaluate the influence of the calculated form drag coefficient on the force balances inside the CFFs at low flow velocities. This was accomplished using the presently developed Computational Fluid Dynamic (CFD) model.

5.2. Computational Fluid Dynamic (CFD) Modelling

The pressure drop over the filter thickness, *i.e.* the pressure difference between the inlet and outlet of the porous media (CFF), was determined, using the developed models, and the results compared to the experimentally measured pressure drop values (ΔP). In Table 2 the average deviation of the modelled pressure drop compared to the experimentally measured are presented. As can be seen from Table 2, both the high and low flow velocity models indicate good agreement with the experimentally measured parameters. The pressure drop obtained from the high flow velocity models showed < ± 1 % deviations from the experimental data. In addition, the low flow velocity models for CFF samples of grade 30, 50 and 65 exhibited ≤ ± 4.6 % deviations from the corresponding empirical data. The model for CFF samples of grade 80 showed the highest deviation, *i.e.* ≤ ± 13.4 %. The overall higher deviation between the modelled and empirical parameters in regards to the low flow velocity results is believed to be due to disturbances in the weight signal originating from the sloshing water in the container on top of the digital scale used (a scale with a resolution of 0.1 mg). As a result, fluctuating data points were obtained and an increased uncertainty in the measured values.

Table 2- The deviation between the modelled and empirical pressure drop data in regards to high and low flow velocity conditions for CFF samples of grade 30, 50, 65 and 80.

Sample No	High Flow Rate Pressure Drop Deviation (Pa) %	Low Flow Rate Pressure Drop Deviation (Pa) %	Sample No	High Flow Rate Pressure Drop Deviation (Pa) %	Low Flow Rate Pressure Drop Deviation (Pa) %
30-1	0.5	1.9	**65-1**	-0.2	0.8
30-2	0.5	-3.3	**65-2**	-0.3	-2.3
30-3	0.9	1.6	**65-3**	-0.4	4.6
50-1	-0.6	-0.8	**80-1**	-0.2	13.4
50-2	-0.3	3	**80-2**	-0.5	-9.6
50-3	0.05	-0.7	**80-3**	-0.4	11.6

In Fig. 4 (a) and (b) the experimental pressure drop over the filter thickness as a function of the fluid velocity for CFF samples of grade 30, 50, 65, and 80, as well as the corresponding results obtained by using the developed models at high and low flow velocities, are presented. As can be seen from the figures, good agreement is obtained between the modelled and experimentally measured values reviling polynomial relations at high flow velocity conditions and linear at low (except for the CFF sample 1 of grade 30 that shows a slight curvature even at low flow velocities as indicated by the oval).

By the use of statistical analysis, it was shown that the differences between the permeability values obtained at high and low flow velocities are insignificant, which again implies that the permeability is not a velocity dependent parameter in the case of porous media. The permeability values for CFF sample 30-1, obtained from high and low flow velocity experiments, were interchanged and the deviation of the model from the experimental results measured. The obtained pressure drop from the high and low flow velocity models proved to deviate 1.2 % and -8.5 % respectively from the corresponding empirically obtained data which is comparable to the pressure drop deviations between the model and experiments for CFF sample 30-1 (0.5 and 1.9 %) presented in Table 1. This further supports the independence of the permeability of a porous media from the intrinsic fluid velocity.

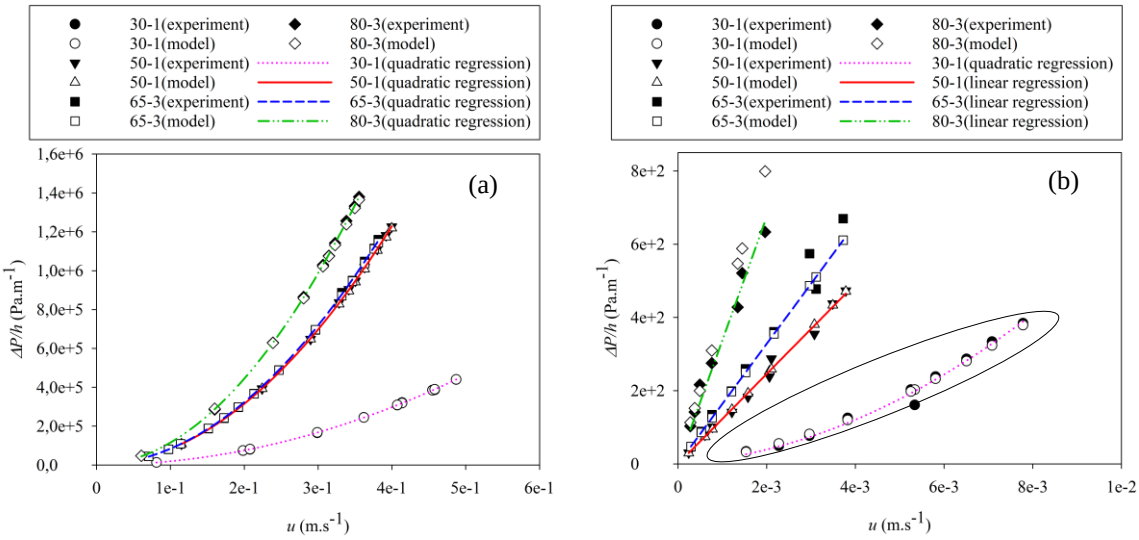

Fig. 4- The experimental pressure drop over the filter thickness as a function of fluid velocity of CFF samples of grade 30, 50, 65, and 80, as well as the corresponding results from the model at high and low flow velocities. (a) High flow velocity conditions, and (b) low flow velocity conditions.

Testing the influence of the drag form coefficients, determined in the pressure drop experiments at low fluid velocity, on the dissipation of the energy was fulfilled by deactivating the Forchheimer drag coefficient, β_F, in the model and calculating the deviation of the obtained pressure drop from the corresponding experimental results. In Fig. 5 the deviation of the modelled pressure drop as a function of the superficial velocity, *i.e.* the linear regression line, for CFF sample 30-1, with deactivated Forchheimer drag coefficient from the corresponding experimental results, i.e. the second order polynomial regression line, is shown.

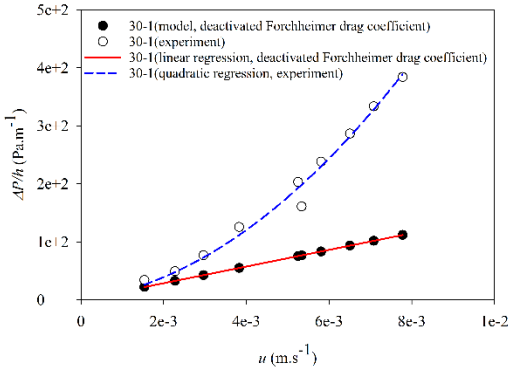

Fig. 5- The difference between the simulated pressure gradient, *ΔP/h*, as a function of superficial velocity, *u*, for CFF sample 30-1 calculated with a deactivated Forchheimer drag coefficient using the developed CFD model from the corresponding experimental results.

As can be seen in Fig. 5, a significant reduction in pressure drop (≈ 80 % if the average deviation of the modelled pressure drop is calculated from the corresponding experimental results) happened by deactivating the Forchheimer drag coefficient which explains the significance influence that the from drag coefficient has on the kinetic energy losses inside the CFF. In other words, the higher velocity range at which the experiments actually were performed, i.e. 1.5-7.7 mm·s^{-1}, is believed to be the primary reason for the higher deviation between the empirical and modelled pressure drop parameters for CFF sample 30-1 at low flow velocity. In the case of the pressure drop results calculated at low flow velocities for CFF samples 50-1 and 65-3, with deactivated Forchheimer drag coefficient, reviles a deviation of 0.8 % and 2.3 % respectively in regards to the empirical parameters (see Fig. 4 (b)). This indicates that the form drag coefficients do not significantly influence the results in these cases, *i.e.* it has an insignificant influence on the dissipation of energy inside the porous media (CFF) compared to the permeability and can be ignored.

6. Conclusion

The pressure and velocity magnitude inside "smooth" water pipes and Al_2O_3-based CFFs of grades 30, 50, 65 and 80 were modelled using a 2D axisymmetric model developed using COMSOL Multiphysics® version 5.3. Permeability and form drag coefficients determined empirically from pressure drop experiments were validated by using the developed model.

The developed CFD models showed a good fit with the pressure drop experiments both at high and low flow velocities. However, the low flow velocity models showed slightly higher deviation from the experimental results, which is believed to be connected to higher experimental uncertainties. The pressure drop obtained from the model for CFF grade 80 proved to have the highest deviation from the empirical pressure drop results, which is believed to be due to high experimental errors.

The specific permeability showed a decrease during low flow velocity measurements compared to the obtained results during high flow measurements, but the statistical analysis along with the developed CFD models showed that the difference between the permeability parameters at high and low flow velocities is insignificant.

The form drag coefficients exhibited also a decrease, but in this case it was determined that the parameter should be considered in view of the pore size of the CFF and over the specific velocity range of interest.

7. AKNOLWDEMENTS

This publication has been funded by the SFI Metal Production, (Centre for Research-based Innovation, 237738). The authors gratefully acknowledge the financial support from the Research Council of Norway and the partners of the SFI Metal Production.

8. REFERENCES

[1] S. Bao, Filtration of aluminium-experiments, wetting and modelling, 2011, p. 204.

[2] M.W. Kennedy, K.X. Zhang, R. Fritzsch, S. Akhtar, J.A. Bakken, R.E. Aune, Characterization of Ceramic Foam Filters Used for Liquid Metal Filtration, Metall Mater Trans B 44(3) (2013) 671-690.

[3] B. Dietrich, W. Schabel, M. Kind, H. Martin, Pressure drop measurements of ceramic sponges-Determining the hydraulic diameter, Chem Eng Sci 64(16) (2009) 3633-3640.

[4] S. Akbarnejad, L.T.I. Jonsson, M.W. Kennedy, R.E. Aune, P.G. Jonsson, Analysis on Experimental Investigation and Mathematical Modeling of Incompressible Flow Through Ceramic Foam Filters, Metall Mater Trans B 47(4) (2016) 2229-2243.

[5] M.W. Kennedy, K. Zhang, J.A. Bakken, R.E. Aune, Determination and Verification of the Forchheimer Coefficients of Ceramic Foam Filters Using COMSOL CFD Modelling COMSOL, Milan, 2012.

[6] H. Huang, J. Ayoub, Applicability of the Forchheimer equation for non-Darcy flow in porous media, Spe J 13(1) (2008) 112-122.

[7] D.B. Ingham, I.I. Pop, Transport phenomena in porous media, Pergamon, Oxford; Danvers, MA, 1998.

[8] J. Bear, Dynamics of fluids in porous media, Dover Publications, New York, N.Y., 1988.

[9] D.A. Nield, A. Bejan, A.G. Springer International Publishing, Convection in porous media, (2017).

[10] W.P. Breugem, The effective viscosity of a channel-type porous medium, Phys Fluids 19(10) (2007).

[11] S. Akbarnejad, M.S. Pour, L.T.I. Jonsson, P.G. Jonsson, Effect of Fluid Bypassing on the Experimentally Obtained Darcy and Non-Darcy Permeability Parameters of Ceramic Foam Filters, Metall Mater Trans B 48(1) (2017) 197-207.

[12] F.M. White, Fluid Mechanics, McGraw-Hill2011.

[13] N.J. Themelis, Transport and Chemical Rate Phenomena, Gordon and Breach, Basel, 1995.

[14] B. Baldwin, H. Lomax, Thin-layer approximation and algebraic model for separated turbulentflows, 16th Aerospace Sciences Meeting, American Institute of Aeronautics and Astronautics1978.

[15] D.B. Ingham, I. Pop, Transport Phenomena in Porous Media, Elsevier Science Ltd1998.

[16] N. Dukhan, O. Bagci, M. Ozdemir, Experimental flow in various porous media and reconciliation of Forchheimer and Ergun relations, Exp Therm Fluid Sci 57 (2014) 425-433.

[17] K. Boomsma, D. Poulikakos, The effects of compression and pore size variations on the liquid flow characteristics in metal foams, J Fluid Eng-T Asme 124(1) (2002) 263-272.